

# Multi-modal diffeomorphic registration using mutual information: Application to the registration of CT and MR pulmonary images.

Laurent Risser<sup>1,2</sup>, Mattias P. Heinrich<sup>1</sup>, Daniel Rueckert<sup>2</sup> and Julia A. Schnabel<sup>1</sup>

<sup>1</sup> Institute of Biomedical Engineering, University of Oxford, Oxford, UK.

{laurent.risser,mattias.heinrich,julia.schnabel}@eng.ox.ac.uk \*

<sup>2</sup> Biomedical Image Analysis Group, Imperial College London, London, UK

D.Rueckert@imperial.ac.uk

**Abstract.** In this paper, we present a new algorithm to register multi-modal images using mutual information in a fully diffeomorphic framework. Our driving motivation is to define a one-to-one mapping in CT/MR 3D pulmonary images acquired from patients with empyema. Due to the large amount of respiratory motion and the presence of strong pathologies, preserving the invertibility of the deformations can be challenging using non-diffeomorphic registration, but would be ensured using a diffeomorphic registration approach. Our main contribution is to propose a computationally tractable technique to estimate the gradients of mutual information in this context. This task can be particularly time consuming since the gradients of mutual information are computed voxel-wise but depend on the information contained in the whole images. Our strategy is then integrated into the Log-Domain Diffeomorphic Demons formalism, making it the first method simultaneously using exponential maps to encode the deformations and mutual information to compare the images. We finally test the whole algorithm on seven CT/MR image volumes of the chest. Results show that the estimated deformations are similar to those obtained using free-form deformations, with the additional property to always estimate invertible deformations.

## 1 Introduction

Image registration is a key step in medical image analysis. In particular, diffeomorphic registration has gained an increasing interest in this community, as it ensures the invertibility and smoothness of the deformations. Among the recent techniques for diffeomorphic registration, the LDDMM formalism [3] encodes the image deformations in time-dependent velocity fields which allows to encode a large range of 3D deformations. An important class of diffeomorphic registration techniques based on stationary velocity fields has also emerged with [1].

---

\* LR and JAS would like to acknowledge funding from EPSRC EP/H050892/1 and the Cancer Research UK / EPSRC Oxford Cancer Imaging Centre (OCIC). MPH is funded by OCIC.

Although such techniques cannot theoretically estimate the same range of diffeomorphisms as those using time-dependent velocity fields, they were shown to be able to estimate similar deformations [6, 11, 19] and they require less computational resources. However, all the above-mentioned techniques use the sum of squared differences deformations to compare images, thus they are only applicable to single modality images. Interestingly, the popular technique of [2] uses local cross correlation as a similarity measure, which relies on local averages and variances of the grey levels, but not on the grey levels directly. It can therefore successfully perform diffeomorphic registration in some multi-modality problems. It is however unsuitable to the registration of multi-modal images where high intensity gradients represent an information depending on the acquisition modality. Our key motivation is to construct a registration algorithm which allows to register CT/MR pulmonary images with reasonable computational resources and the desirable properties of the diffeomorphic registration algorithms. We therefore use the *LogDemons* formalism [11, 19] because its implementation is simple, it requires the tuning of relatively few parameters, and it computes invertible and smooth deformations with reasonable resources.

In this paper, the amplitude of the *forces* pushing the source image toward the target image is based on the mutual information (MI) between the images [10, 17, 20]. Compared with sum of squared differences, a key advantage of mutual information is that it measures the similarity between the partition of the grey levels in the registered images, and not the similarity between the grey levels directly. It also allows to treat more challenging multi-modal problems than cross-correlation. It has been successfully used in parametric non-rigid registration [8, 16, 17]. It has also been used in extensions of the diffeomorphic demons algorithm [9, 12] which ensures the invertibility of the updates, but **not** the invertibility of the whole deformation as in the LogDemons formalism. Note that contrary to [9, 12], we focus here on the description of an efficient technique for the estimation of the MI gradients. In our approach, the *forces* are based on the information contained in the whole images and are applied pointwise. Our approach therefore presents strong similarities with the non-diffeomorphic registration algorithms of [5, 15] but differs from [4] which uses adaptive local mutual information. In [5] the authors compute local gradients of an energy depending on the mutual information and post-filtering the normalised joint histogram of the image intensities. This however lowers the intensity sensitivity. Our approach is closer to [15], where the gradients of multi-modal similarity measures, also based on joint intensities, are not smoothed. We however develop our framework in the context of diffeomorphic registration. Note finally that the recent approach of [13], which uses time dependent velocity fields and normalised mutual information may show similarities with the method proposed here.

The paper is organised as follow: We first give an overview of the LogDemons algorithm. We then interpret the equations developed in [17] to estimate voxel-wise gradients of mutual information at a low computational cost and integrate these gradients in the LogDemons framework. Our algorithm is finally compared

quantitatively with the free-form deformations algorithm [16], which also uses mutual information, on seven multi-modal MR/CT 3D images of the chest.

## 2 Overview of the Log-Domain Diffeomorphic Demons

In this section, we give an overview of the LogDemons framework [19]. Let  $I_S$  be a source image defined on the spatial domain  $\Omega \subset \mathbb{R}^n$  and registered on a target image  $I_T \in \Omega$ . Here,  $I_S$  is transformed through the time-dependent diffeomorphic transformation  $\phi_t^v$ ,  $t \in [0, 1]$  which is defined by a stationary velocity field  $v$  using:  $\frac{\partial}{\partial t} \phi_t^v = v(\phi_t^v)$ , where  $\phi_0^v = \text{Id}$ . The final deformation is the exponential map of  $v$ ,  $\exp(v) \doteq \phi_1^v$ , and the deformed source image is then computed as  $I_S \circ \exp(v)$ . The optimal velocity field  $\tilde{v}$  is obtained by minimizing  $\tilde{v} = \arg \min_v E(v, v_c)$ , where the energy  $E$  is defined as:

$$E(v, v_c) = \frac{1}{\lambda_i^2} \|I_T - I_S \circ \phi_1^{v_c}\|_{L^2}^2 + \frac{1}{\lambda_x^2} \|\log((\phi_1^v)^{-1} \circ \phi_1^{v_c})\|_{L^2}^2 + \frac{1}{\lambda_d^2} \|\nabla v\|_{L^2}^2 \quad (1)$$

where the logarithm is the inverse operation of the exponential. In this equation, the first term measures the sum of squared differences between the registered image intensities, the second term measures the correspondence between the smooth deformation  $\phi_1^v$  and the deformation  $\phi_1^{v_c}$ , and the third term measures the spatial regularity of  $v$ . Insights about the influence of the parameters  $\lambda_i$ ,  $\lambda_x$ ,  $\lambda_d$  are thoroughly developed in [11]. A key aspect of the demons algorithms is that it decouples the estimation of the optimal image matching (terms 1 and 2 of Eq. (1)) with the spatial regularisation of the deformations (terms 2 and 3 of Eq. (1)). As a result, the velocity field  $v_c$  encodes an intermediate transformation  $\phi_1^{v_c}$ , called correspondence, which matches the two images without considering the regularity of the transformation. Minimisation of  $E(v, v_c)$  is as follows: The velocity field  $v$  is initialised as null. Then  $E(v, v_c)$  is iteratively minimised using a two sub-step strategy: Firstly,  $v_c$  is computed using  $v$  and an update field  $\delta v$ , defined as:

$$\delta v(x) = -\frac{I_T - I_S \circ \phi_1^v}{\|\mathbf{J}(x)\|^2 + \lambda_i^2/\lambda_x^2} \mathbf{J}(x) \quad (2)$$

where  $\mathbf{J}(x)$  is the gradient of the image intensities,  $\mathbf{J}(x) = \nabla(I_S \circ \phi_1^v)$ . Note that  $\delta v$  may be smoothed by a Gaussian kernel (fluid-like regularisation). Ideally,  $v_c$  should be updated using  $v_c = \log(\phi_1^v \circ \phi_1^{\delta v})$ . Since the logarithm of a deformation is computationally intractable in general,  $v_c$  is approximated using the Baker-Campbell-Hausdorff (BCH) formula:  $v_c \simeq v_c + \delta v + [v, \delta v]/2 + [v, [v, \delta v]]$ , where the Lie bracket  $[., .]$  is defined by  $[v_1, v_2] = (\nabla v_1)v_2 - (\nabla v_2)v_1$ . In the second sub-step,  $v$  is updated by smoothing  $v_c$  using a Gaussian kernel (diffusion like regularisation).

### 3 Approximating the mutual information gradient

Let  $\omega_S$  and  $\omega_T$  be two Parzen windows that are related to the intensities of  $I_S \circ \phi_1^Y$  and  $I_T$ . As in [17], we build the Parzen windows using cubic B-splines so that they have unit integral and respect the partition unity. The discrete sets of intensities associated with  $I_S \circ \phi_1^Y$  and  $I_T$  are  $L_S$  and  $L_T$ , respectively. The joint Parzen discrete probability between  $I_S \circ \phi_1^Y$  and  $I_T$  is then:

$$p(i, j; \mathbf{v}) = \frac{\alpha(\mathbf{v})}{\epsilon_S \epsilon_T} \sum_{\mathbf{x} \in \Omega} \omega_S \left( \frac{i - I_S \circ \phi_1^Y(\mathbf{x})}{\epsilon_S} \right) \omega_T \left( \frac{j - I_T(\mathbf{x})}{\epsilon_T} \right), \quad (3)$$

where  $i \in L_S$ ,  $j \in L_T$ ,  $\epsilon_T$  and  $\epsilon_S$  are scaling factors controlling the size of the Parzen windows, and  $\alpha(\mathbf{v})$  is the normalizing constant of the probabilities. The marginal discrete probabilities are then  $p_S(i; \mathbf{v}) = \sum_{j \in L_T} p(i, j; \mathbf{v})$  and  $p_T(j; \mathbf{v}) = \sum_{i \in L_S} p(i, j; \mathbf{v})$ . Since  $I_T$  is the fixed image, the probabilities  $p_T$  do not depend on  $\mathbf{v}$ . We then denote  $p_T(j; \mathbf{v}) = p_T(j)$ . The mutual information between  $I_S \circ \phi_1^Y$  and  $I_T$  is then:

$$S(\mathbf{v}) = - \sum_{i \in L_S} \sum_{j \in L_T} p(i, j; \mathbf{v}) \log_2 \left( \frac{p(i, j; \mathbf{v})}{p_S(i; \mathbf{v}) p_T(j)} \right) \quad (4)$$

#### 3.1 Analytical estimation of the mutual information gradient

In [17] the authors show that when only the source image is deformed to match the target image, the derivative of the mutual information  $S$  according to a deformation parameter  $\mu$  can be written as:

$$\frac{\partial S}{\partial \mu} = - \sum_{i \in L_S} \sum_{j \in L_T} \frac{\partial p(i, j; \mathbf{v})}{\partial \mu} \log_2 \left( \frac{p(i, j; \mathbf{v})}{p_S(i; \mathbf{v})} \right) \quad (5)$$

and develop this equation in the context of parametric registration. It is however interesting to note that this equation is sufficiently general to model  $\mu$  as any deformation of  $\phi_1^Y$ . We then compute the derivative of  $p(i, j; \mathbf{v})$  according to  $\mu$ :

$$\begin{aligned} \frac{\partial p(i, j; \mathbf{v})}{\partial \mu} &= a_1 \sum_{\mathbf{x} \in \Omega} \frac{\partial \omega_S \left( \frac{i - I_S \circ \phi_1^Y(\mathbf{x})}{\epsilon_S} \right)}{\partial \mu} \omega_T \left( \frac{j - I_T(\mathbf{x})}{\epsilon_T} \right) \\ &= \frac{-a_1}{\epsilon_S} \sum_{\mathbf{x} \in \Omega} \frac{\partial I_S \circ \phi_1^Y(\mathbf{x})}{\partial \mu} \left. \frac{\partial \omega_S(\xi)}{\partial \xi} \right|_{\xi=\frac{i - I_S \circ \phi_1^Y(\mathbf{x})}{\epsilon_S}} \omega_T \left( \frac{j - I_T(\mathbf{x})}{\epsilon_T} \right) \end{aligned}$$

where  $a_1$  is constant for all intensity levels  $i$  and  $j$ . Eq. (5) can then be written:

$$\begin{aligned} \frac{\partial S}{\partial \mu} &\sim \\ &\sum_{\mathbf{x} \in \Omega} \sum_{i \in L_S} \sum_{j \in L_T} \frac{\partial I_S \circ \phi_1^Y}{\partial \mu} \left. \frac{\partial \omega_S(\xi)}{\partial \xi} \right|_{\xi=\frac{i - I_S \circ \phi_1^Y(\mathbf{x})}{\epsilon_S}} \omega_T \left( \frac{j - I_T(\mathbf{x})}{\epsilon_T} \right) \log_2 \left( \frac{p(i, j; \mathbf{v})}{p_S(i; \mathbf{v})} \right) \end{aligned} \quad (6)$$

The third and fourth terms of Eq. (6) can be straightforwardly computed from the current deformation. The second one can also be analytically computed since the  $\omega_S$  is constructed using B-splines. The first term however depends on the type of deformation that  $\mu$  represents. Importantly, the derivative  $\partial S / \partial \mu$  is computed using a triple-sum on  $\Omega$ ,  $L_S$  and  $L_T$ , which is critical in terms of computational burden in the general case. We propose in the next subsection a new strategy to locally estimate the derivative of Eq. (6) in the framework of the LogDemons at a low algorithmic cost.

### 3.2 Approximation of the mutual information gradient

As introduced earlier, in the LogDemons framework, the update field  $\delta\mathbf{v}$  is computed without considering the regularity of the transformation. When estimating  $\delta\mathbf{v}$  in the point  $\mathbf{x} \in \Omega$  using Eq. (6), we consider the parameter  $\mu_{\mathbf{x}}$  as a local translation of  $\mathbf{x}$  and do not perform any image or histogram smoothing. In addition, the local updates are constructed in the direction of the intensity gradients with an amplitude depending almost exclusively on the mutual information. To do so, we denote  $\mathbf{b}(\mathbf{x}) = \frac{\nabla I_S \circ \phi_1^Y(\mathbf{x})}{|\nabla I_S \circ \phi_1^Y(\mathbf{x})|}$  as the normalised intensity gradient and consider the points  $\mathbf{x}_n = \mathbf{x} + n\delta\mathbf{b}$ ,  $n \in \{-1, 0, 1\}$ , where  $\delta$  is the spatial distance between the points  $\mathbf{x}_n$ . We also reduce the number of bins  $i$  and  $j$  considered in Eq. (6) by exploiting the fact that the cubic B-splines in  $\omega_S$  and  $\omega_T$  (cf. beginning of section 3) are non-null on a compact domain only. To do so, we first denote  $\gamma$  this domain's extent. We then denote  $L_{S,\mathbf{x}}$  and  $L_{T,\mathbf{x}}$ , the subsets of  $L_S$  and  $L_T$  representing bins with less intensity difference than  $\gamma$  with  $I_S \circ \phi_1^Y(\mathbf{x}_n)$  and  $I_T(\mathbf{x})$  respectively. We then estimate the contribution of the points  $\mathbf{x}_n$  to the mutual information  $S$  using:

$$S(\mathbf{x}) = \sum_{\mathbf{x}_n} \sum_{i \in L_{S,\mathbf{x}_n}} \sum_{j \in L_{T,\mathbf{x}_n}} I_S \circ \phi_1^Y(\mathbf{x}_n) \left. \frac{\partial \omega_S(\xi)}{\partial \xi} \right|_{\xi = \frac{i - I_S \circ \phi_1^Y(\mathbf{x}_n)}{\epsilon_S}} \omega_T \left( \frac{j - I_T(\mathbf{x}_n)}{\epsilon_T} \right) \log_2 \left( \frac{p(i, j; \mu)}{p_S(i; \mu)} \right) \quad (7)$$

and the contribution  $S^+(\mathbf{x})$  and  $S^-(\mathbf{x})$ , if the points points  $\mathbf{x}_n$  are translated by  $\delta\mathbf{b}$ , and by  $-\delta\mathbf{b}$ . The corresponding contributions are obtained by replacing  $\mathbf{x}_n$  by  $\mathbf{x}_n - \delta\mathbf{b}$  and  $\mathbf{x}_n + \delta\mathbf{b}$  in the first term of Eq. (7). In the present context, the derivative Eq. (6) is then estimated in the direction where the variation of mutual information is the highest:

$$\frac{\partial S}{\partial \mu_{\mathbf{x}}}(\mathbf{x}) \sim \min \left( \frac{S^+(\mathbf{x}) - S(\mathbf{x})}{\delta}, \frac{S^-(\mathbf{x}) - S(\mathbf{x})}{\delta} \right) \quad (8)$$

Note that the minimum value is considered because the values of  $S$ ,  $S^+$  and  $S^-$  are negative. Using this strategy, only five trilinear interpolations of the grey levels in  $I_S \circ \phi_1^Y$  are required to estimate  $\partial S(\mathbf{x}) / \partial \mu_{\mathbf{x}}$ , this simple operation being the most demanding in terms of computational resources.

### 3.3 Mutual information based Log-Demons

In order to perform diffeomorphic image registration using mutual information, we use the same algorithm as [19], but with a different definition of the update fields  $\delta\mathbf{v}$ . For each point  $\mathbf{x} \in \Omega$ , we consider the gradient  $\mathbf{G}(\mathbf{x}) = \nabla I_S \circ \phi_1^Y(\mathbf{x})$  and the derivative  $\frac{\partial S}{\partial \mu_{\mathbf{x}}}(\mathbf{x})$  of Eq. 8. By adapting the forces of [18] to our framework, we propose to use the following local updates  $\delta\mathbf{v}(\mathbf{x})$ :

$$\delta\mathbf{v}(\mathbf{x}) = \frac{\frac{\partial S}{\partial \mu_{\mathbf{x}}}(\mathbf{x})}{|\mathbf{G}(\mathbf{x})| + \frac{|\frac{\partial S}{\partial \mu_{\mathbf{x}}}(\mathbf{x})|}{\sigma_x}} \mathbf{G}(\mathbf{x}),$$

where  $\sigma_x$  controls the maximum update length per iteration. Even though the direction of the updates depends on the intensity gradients, their amplitude is then strongly related to the local variation of mutual information.

## 4 Results

In this section, we evaluate the proposed method on seven multi-modal CT/MR 3D images acquired on patients suffering from empyema. This disease is an infection of the lung pleura which implies an excess fluid to fill up the pleural space (pleural effusion). The fluid turns into an abscess and it can cause the lung to collapse. CT and MR modalities are useful to detect empyema. Non-rigid deformations are observed between the CT and MR images since the patients are scanned in two different sessions and at different levels of breath-hold. A non-rigid alignment of both modalities has a great potential to support the diagnostic task. Due to the presence of strong pathologies and the relatively large amplitude of the respiratory motion, ensuring the one-to-one mapping between the CT and MR images can be challenging by using non-diffeomorphic registration techniques. The proposed fully diffeomorphic strategy therefore makes sense in this context since it ensures this one-to-one mapping.

The scans are acquired using different anisotropic voxel sizes, so all images are resampled to voxels of size  $1.5 \times 1.5 \times 2.5$  mm using trilinear interpolation. Note that a particular challenge for the registration here is the large slice thickness of up to 8 mm in the original MR images. For each patient, we first denoised the images using anisotropic diffusion [14], performed a rigid alignment of the images and defined region of interests of about  $280 \times 280 \times 130$  voxels in the CT and MR images. We then performed non-rigid registration between the 3D images by using mutual information LogDemons (MI-LogDemons). For comparison purpose, we also used the free-form deformation algorithm of [16]<sup>3</sup>, as it was one of the best-performing algorithms in [7]. For both algorithms, we used 40 bins to compute the intensity histograms and multi-resolution schemes with 3 resolution levels. We used default parameters with the FFD algorithm. For the MI-LogDemons algorithm, the fluid- and diffusion-like regularisation was respectively performed using Gaussian kernels of  $\{40, 20, 10\}$ mm and  $\{1, 1, 1\}$ mm at

---

<sup>3</sup> <http://www.doc.ic.ac.uk/~dr/software/>

{quarter, half, full} resolution. Due to the large slice thicknesses, common landmarks in the CT/MR images cannot be defined with enough spatial accuracy to allow pertinent comparisons of the registered images. In lack of any other gold standard, the registration quality is therefore assessed by comparing the mutual information (MI) between the MR image and the CT image after registration. The ability to compute invertible deformations is also measured using the percentage of voxels with negative Jacobians in the estimated displacement fields. Quantitative results are given in Table 1. The matching quality is also illustrated in Fig. 1. Note that the registration is performed in 3D, hence small out-of-plane deformations may be interpreted as large deformations in the observed slices. Note also that the lower the mutual information, the more accurate the matching.

**Table 1. (Top)** Mutual information between the MR and CT images aligned using rigid registration (Rigid Reg.), free-form deformations [16] (FFD) and Mutual Information LogDemons (MI-LogD) in seven patients. **(Bottom)** Percentage of voxels with negative Jacobians in the corresponding deformations.

		Pat. 1	Pat. 2	Pat. 3	Pat. 4	Pat. 5	Pat. 6	Pat. 7
MI-Info.	Rigid Reg.	-0.41	-0.10	-0.34	-0.34	-0.47	-0.57	-0.44
	FFD	-0.48	-0.14	-0.42	-0.51	-0.73	-0.71	-0.69
	MI-LogD	-0.61	-0.15	-0.41	-0.54	-0.72	-0.75	-0.79
Std J	FFD	0.30	0.35	0.27	0.21	0.28	0.36	0.39
	MI-LogD	0.35	0.39	0.41	0.23	0.37	0.45	0.42
%J<0	FFD	1.49	0.042	0.048	1.08	0.001	0.095	0.057
	MI-LogD	0	0	0	0	0	0	0

In our results, the quality of the registration obtained using FFD is slightly better to the one obtained using MI-LogDemons with slightly more flexibility. These differences may be due to the parameterisation of the algorithms. By using both techniques, Table 1 and Fig. 1 also show an obvious improvement of the structures alignment compared with rigid registration. Importantly, no negative Jacobians were computed using MI-LogDemons, and up to 1.49 % of pixels with negative Jacobians were estimated using FFD. This is due to the diffeomorphic properties of the MI-LogDemons which ensure the estimation of one-to-one mappings. Obviously, it would be possible to use hard constrains or more regularisation with the FFD algorithm but this would penalise the flexibility of the deformations. In terms of time of computations, the MI-LogDemons registration required about 40 minutes while FFD required about 4 hours to register each pair of CT/MR images<sup>4</sup>. Note finally that in our tests, even though

<sup>4</sup> C++ language on an iMac with 2.93GHz Intel Core i7 and 8 GB memory

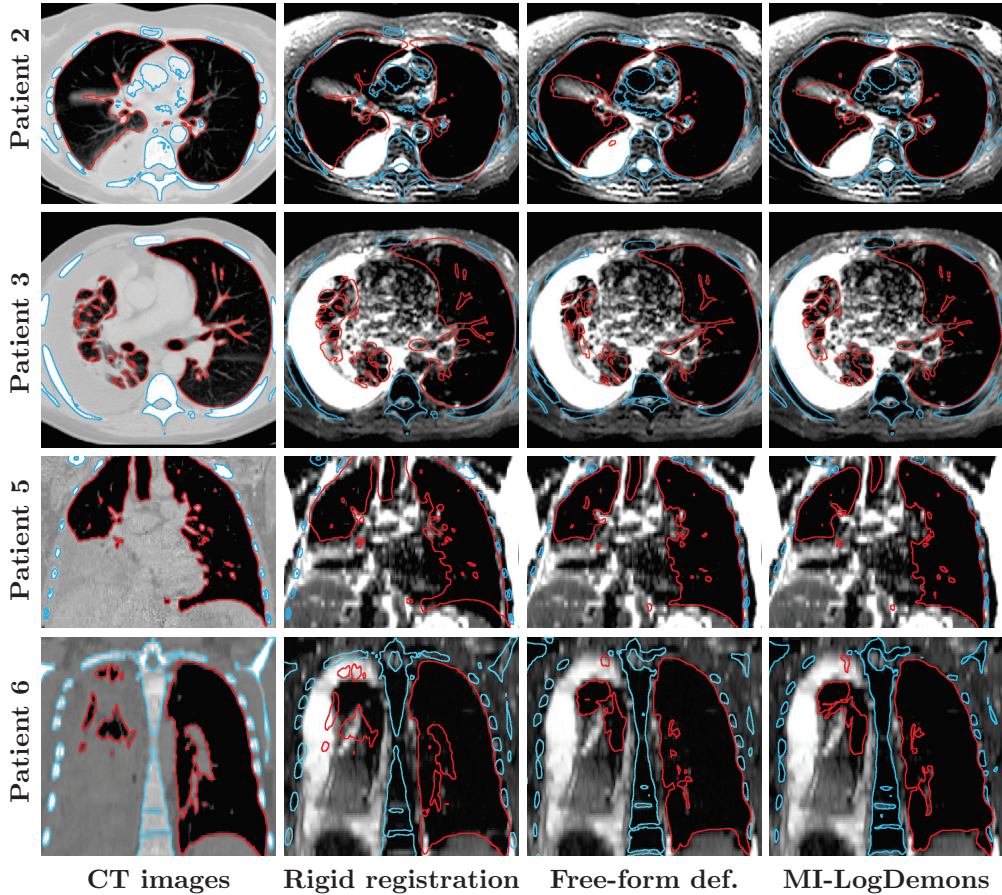


**Fig. 1.** Multi-modal registration of 3D CT/MR images of the lungs using rigid registration, free-form deformations [16] and Mutual Information LogDemons. The curves in blue and red represent two isolines in the CT images. They are deformed using the estimated deformation from the CT images to the MR images.

the gradients are computed locally, the MI-LogDemons algorithm shows little sensitivity to partial volume effects. This may be due to the use of a gradually decreasing amount of smoothing during the registration.

## 5 Conclusion

We have introduced MI-LogDemons as a powerful tool for diffeomorphic registration of multi-modal images. In our tests, it has estimated similar deformations

as by using the standard multi-modal registration algorithm of [16]. In addition, it ensured the one-to-one mapping of the deformations, which is important in the clinical problem addressed. By using non-diffeomorphic approaches [8, 16, 17], or approaches in which only the update fields are diffeomorphic [9, 12], such properties could otherwise be only ensured by using hard-constraints which reduce the possible range of deformations to match the images. Note that the use of a deformation flow instead of a displacement map also opens new research directions for the comparison of multimodal images. Importantly, the proposed method as a whole is finally not very demanding in terms of computational resources.

## References

1. Arsigny, V., Commowick, O., Pennec, X., Ayache, N.: A log-Euclidean framework for statistics on diffeomorphisms. In: Proceedings of MICCAI. pp. 924–931. No. 4190 (2006)
2. Avants, B.B., Epstein, C.L., Grossman, M., Gee, J.C.: Symmetric diffeomorphic image registration with cross-correlation: Evaluating automated labeling of elderly and neurodegenerative brain. Medical Image Analysis 12, 26–41 (2008)
3. Beg, F.M., Miller, M.I., Trouvé, A., Younes, L.: Computing large deformation metric mappings via geodesic flows of diffeomorphisms. International Journal of Computer Vision 61(2), 139–157 (February 2005)
4. De Nigris, D., Mercier, L., Del Maestro, R., Collins, D.L., Arbel, T.: Hierarchical multimodal image registration based on adaptive local mutual information. In: MICCAI (2). pp. 643–651 (2010)
5. Hermosillo, G., Chefd'hotel, C., Faugeras, O.: Variational methods for multimodal image matching. International Journal of Computer Vision 50(3), 329–343 (2002)
6. Hernandez, M., Bossa, M.N., Olmos, S.: Registration of anatomical images using paths of diffeomorphisms parameterized with stationary vector field flows. International Journal of Computer Vision 85(3), 291–306 (2009)
7. Klein, A., Andersson, J., Ardekani, B.A., Ashburner, J., Avants, B., Chiang, M.C., Christensen, G.E., Collins, D.L., Gee, J., Hellier, P., Song, J.H., Jenkinson, M., Lepage, C., Rueckert, D., Thompson, P., Vercauteren, T., P. Woods, R., Mann, J., V. Parseya, R.: Evaluation of 14 nonlinear deformation algorithms applied to human brain MRI registration. NeuroImage 46(3), 786–802 (July 2009)
8. Loeckx, D., Slagmolen, P., Maes, F., Vandermeulen, D., Suetens, P.: Nonrigid image registration using conditional mutual information. IEEE Trans. Med. Imaging 29, 19–29 (2010)
9. Lu, H., Reyes, M., Šerijović, A., Weber, S., Sakurai, Y., Yamagata, H., Cattin, P.C.: Multi-modal diffeomorphic demons registration based on point-wise mutual information. In: Proceedings of ISBI. pp. 372–375. (2010)
10. Maes, F., Collignon, A., Vandermeulen, D., Marchal, G., Suetens, P.: Multimodality image registration by maximization of mutual information. IEEE Trans. Med. Imaging 16(2), 187–198 (1997)
11. Mansi, T., Pennec, X., Sermesant, M., Delingette, H., Ayache, N.: iLogDemons: A demons-based registration algorithm for tracking incompressible elastic biological tissues. International Journal of Computer Vision 92(1), 92–111 (2011)
12. Modat, M., Vercauteren, T., Ridgway, G.R., Hawkes, D.J., Fox, N.C., Ourselin, S.: Diffeomorphic demons using normalized mutual information, evaluation on multimodal brain MR images. In: Proceedings of SPIE Medical Imaging - Image Processing. pp. 13–18 (2010)

13. Modat, Ridgway, G.R., Daga, P., Cardoso, M.J., Hawkes, D.J., Ashburner J., Ourselin, S.: Log-Euclidean free-form deformation. In: Proceedings of SPIE Medical Imaging - Image Processing. (2011)
14. Perona, P., Malik, J.: Scale-space and edge detection using anisotropic diffusion. *IEEE Transactions on Pattern Analysis and Machine Intelligence* 12(7), 629–639 (1990)
15. Rogelj, P., Kovačič, S., Gee, J.C.: Point similarity measures for non-rigid registration of multi-modal data. *Comp. Vis. Understanding* 92, 112–140 (2003)
16. Rueckert, D., Sonoda, L.I., Hayes, C., Hill, D.L.G., Leach, M.O., Hawkes, D.J.: Nonrigid registration using free-form deformations: Application to breast MR images. *IEEE Trans. Med. Imaging* 18(8), 712–721 (1999)
17. Thévenaz, P., Unser, M.: Optimization of mutual information for multiresolution image registration. *IEEE Trans. Imag. Proc.* 9(12), 2083–2099 (2000)
18. Thirion, J.P.: Non-rigid matching using demons. In: Proceedings of the Conference on Computer Vision and Pattern Recognition (CVPR). p. 245 (1996)
19. Vercauteren, T., Pennec, X., Perchant, A., Ayache, N.: Symmetric log-domain diffeomorphic registration: A demons-based approach. In: Proceedings of MICCAI. pp. 754–761 (2008)
20. Viola, P.A., Wells, W.M.: Alignment by Maximization of Mutual Information. In: Proceedings of ICCV. pp. 16–23 (1995)